Research Journal of Applied Sciences, Engineering and Technology 7(1): 137-143, 2014
DOI:10.19026/rjaset.7.230
ISSN: 2040-7459; e-ISSN: 2040-7467
© 2014 Maxwell Scientific Publication Corp.
Submitted: February 25, 2013 Accepted: March 29, 2013 Published: January 01, 2014

Research Article

Aerodynamic Performance Research of Chordwise Swept Blade Cascade HP Stage at Off-design Condition

Feng Zi-Ming, Gu Hui-Bin and Ding Huan-Huan
School of Mechanical Science and Engineering, Northeast Petroleum University,
Daqing, Heilongjiang, 163318, China

Abstract: In order to research the chordwise swept cascade stage control mechanism for internal flow field under the off-design condition, the 600 MW supercritical steam turbine HP rotor and static blades were selected as prototypes. The chordwise fore-swept cascade stage and chordwise aft-swept cascade stage were achieved with 30% blade height and 20°, -20° swept angle respectively. The three cascades passage flow numerical simulation was conducted by CFD software. The computed results indicated that the degree of reaction and isentropic efficiency of the three cascade stages were changed very little in the scope of 70~120% design flux and decreased sharply when the inlet flux was less than 50% design flux. On the whole, chordwise fore-swept cascade stage had the best aerodynamic performance.

Keywords: Chordwise swept blade, high pressure stage, numerical simulation, off-design

INTRODUCTION

Turbo machinery was a key component to the devices such as gas turbine, steam turbine and aircraft engine and played an important role in the national economy. The steam turbine's adaptive capacity to bad condition was one of the main performance indexes. So it was a must to deeply research the complex passage flow field of steam turbine cascades and loss mechanisms at off-design condition to explore the ways and means to reduce the cascade flow loss and improve the cascade aerodynamic performance and increase the turbine efficiency. People generally used the traditional boundary layer theory to study the viscous effects and the mechanism of flow loss in the cascade flow field (Ainley, 1948).

When the steam turbine units were working in an off-design condition, the cascade load and blade surface velocity distribution would change very much, especially the leading edge velocity distribution of cascade. If the negative or positive incidence was overlarge, the flow separation would happen at the blade leading edge that would cause a largish flow loss. For any blade profile, there was an optimum incidence (Hournouziadis and Bergmann, 1987), corresponding to the minimum flow loss. There are many research achievement of the flow loss at off-design condition at home and abroad (Solomon, 2000; Jouini and Ajolander, 2000; Willinge and Haselbacher, 2004; Corriveau and Sjolander, 2005; Zoric and Sjolander, 2007). Mayle (1991) considered that under the big incidence condition, the boundary layer separation in the pressure surface would result little supplementary flow loss because of the thin boundary layer in the pressure. At big positive incidence, the boundary layer in the suction surface would be separated and produce a lot of flow loss.

This study used the NUMECA software as computing platform to conduct chordwise fore-swept, chordwise aft-swept and prototype HP stages numerical simulation studied at different flux conditions. The simulation results indicated that the three types of HP stage had very good adaptability to variable flux and the chordwise fore-swept blade cascade stage was especially prominent.

Geometric model and definition of chordwise swept: Using super-critical HP steam stage static blade cascade as the prototype blade and modifying the blade, we can obtain a series of new blade-shape through making the stacking line of gravity fore-sweep and aft-sweep. According to tilt direction of coming flow compared with the leading edge line of blade it can be divided into two kinds of fore-sweep and aft-sweep, fore-sweep means that the leading edge line tilt against the direction of coming flow, on the contrary it is aft-sweep. As show in Fig. 1, A is the sweep angle, LE is the leading edge, TE is the trailing edge, H is the blade height.

Corresponding Author: Feng Zi-Ming, School of Mechanical Science and Engineering, Northeast Petroleum University, Daqing, Heilongjiang, 163318, China
This work is licensed under a Creative Commons Attribution 4.0 International License (URL: http://creativecommons.org/licenses/by/4.0/).

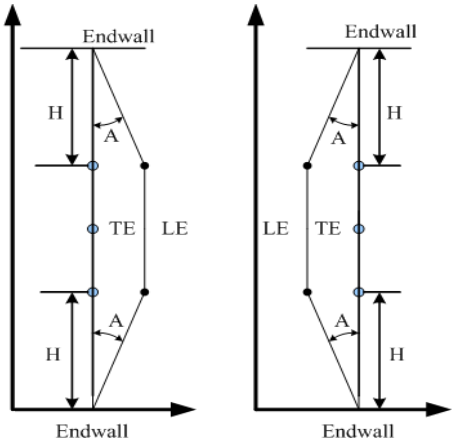

Fig. 1: Chordwise fore-swept and chordwise aft-swept blade

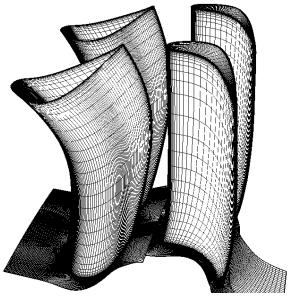

(a) 3D stage grid mesh

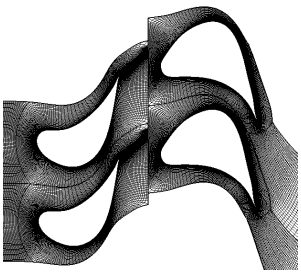

(b) Blade root grid mesh

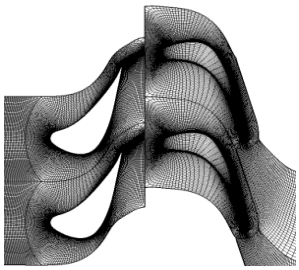

(c) Blade tip grid mesh

Fig. 2: Schematic diagram of 3D computation mesh

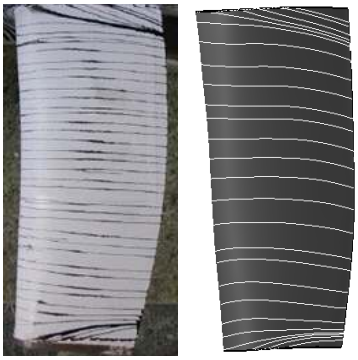

Fig. 3: Streamline of suction surface

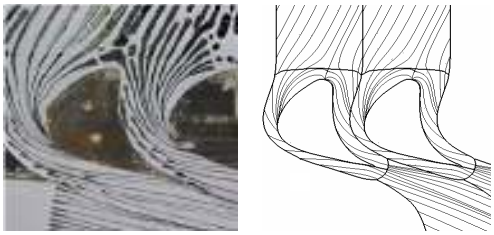

Fig. 4: Streamline of hub

COMPUTING METHOD AND BOUNDARY CONDITIONS

The numerical simulation software was NUMECA. The mesh was generated by Auto Grid and the turbo machinery internal flow simulation was conducted by FINE. The tip and root mesh of cascades were made of H, O, O, I-types as Fig. 2 shown. The static blade cascade inlet mesh was H-type. The passage mesh of static and rotor blade cascades were all O-types. The rotor outlet mesh was I-type. Total mesh nodes were 1.03 million. The inlet total pressure was 5.948 MPa, inlet total temperature was 625 k and outlet static pressure was 5.024 MPa. The rotor rotate speed was 3000 rpm. The outlet boundary conditions were all static pressure value at intermediate diameter location and computed the outlet static pressure radial distribution by simple radial balance equation. Solid wall boundary was adiabatic and no slip boundary condition. S-A model was chosen as turbulence model.

Figure 3 and 4 respectively indicated the comparison of experimental and calculated results of the streamline in suction surface and the down end wall, the calculated results was consistent with the experimental results.

Figure 5 respectively indicated the comparison of experimental and calculated results of the static pressure coefficient of prototype blade cascade at up, middle and down profile surface. As can be seen from Fig. 5, most of the calculated values of the static pressure coefficient were consistent with the rested

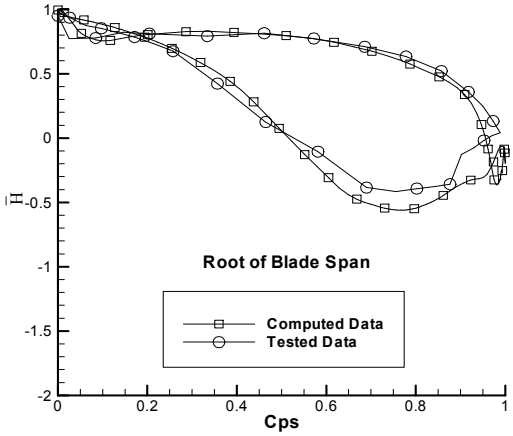

(a) Up of profile

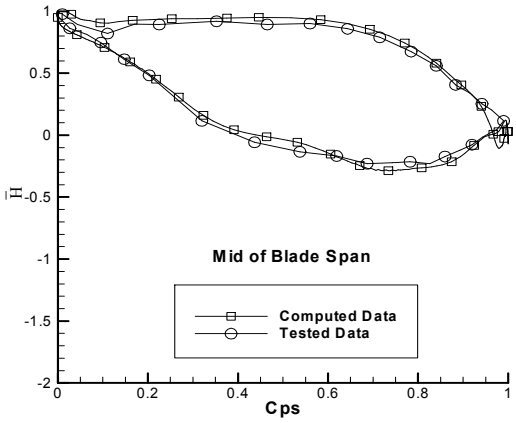

(b) Middle of profile

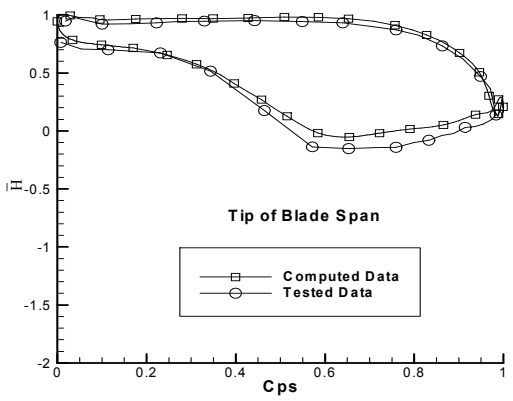

(c) Root of profile

Fig. 5: Static pressure coefficient on blade profile

values in the total profile surface. Taken the test measuring error and calculated error into consideration, the simulation results with NUMECA was credible.

RESULTS AND DISCUSSION

Streamline distribution of HP stage at middle blade span at off-design condition: The streamlines of SWF, PB and SWB cascade at middle blade were shown in Fig. 6. The first column graph were the simulated streamline at design condition, the second column were the simulated streamline at 50% design condition, the third column were the simulated streamline at 35% design condition. The second, fourth and sixth row graph were the partial enlarged drawing of streamline on the rotor pressure side.

At the design condition, the three stages streamline nearly flowed along the blade profile. It was indicated that the middle flow of any type blade profile was laminar flow and there wasn't any secondary flow. When the inlet flux reached 50% design condition, the static cascade streamline still flowed along the blade profile, but the rotor cascade streamline deflected to the rotor suction side and formed negative incidence resulting secondary flow on the pressure side. The vortex of SWB stage was the biggest, followed by PB stage and SWF stage was the last.

When the inlet flux reached 35% design condition, the streamline deflected from leading edge of cascade become longer than before. The vortex on rotor blade increased and strengthened and occupied two-third region of the pressure surface along axial direction. The vortex of SWB stage occupied almost half region between the cross-cascades along axial direction and was bigger than SWF and PB.

Streamline of HP stage blade surface at off-design condition: As could be seen from Fig. 7, at the design condition, the blade passage flow spectrum was relatively simple. The three cascades was two-dimensional flow in most span wise direction and had little change in the blade root. The streamline at the blade tip of SWF rotor flowed along the blade profile curve. The separation line, corresponding to the tip passage vortex, was disappeared and the end wall airflow was rolled up very little to the span wise direction. The rolled-up airflow of SWB up blade was bigger than that of the PB and was reattached in suction surface, then formed reattached line.

In the 50% design flow condition, the internal flow of turbine made a significant change and its streamline in blade surface, with complicated flow spectrum, was different in the design flow condition. suction side, the starting point of the up and down passage vortex's separated line of SWF rotor all moved to the trailing edge, so that the up and down end wall flow properties was improved. But the SWB was to the contrary. In the

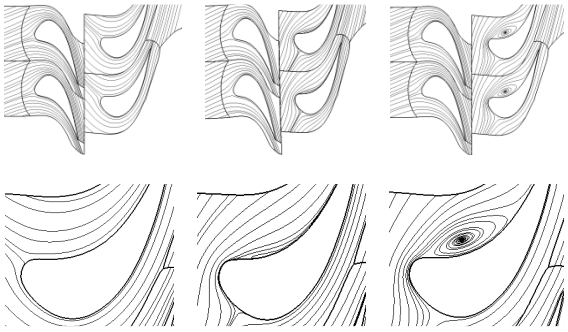

(a) SWF stage mid blade span streamline

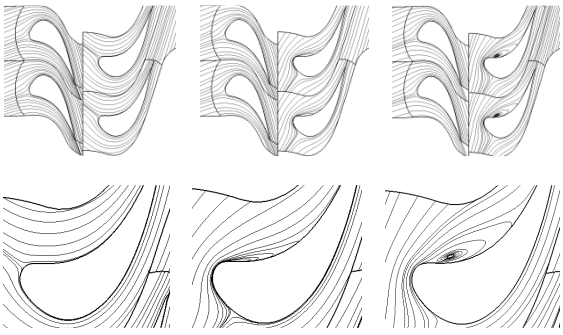

(b) PB stage mid blade span streamline

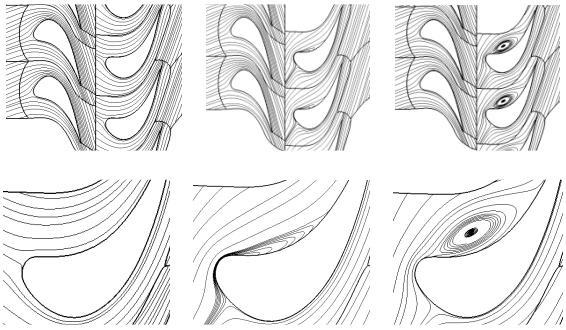

(c) SWB stage mid blade span streamline

Fig. 6: Streamline in the mid span plan of HP stage blade

pressure side of the rotor blade, there was a reattached line corresponding to the separation zone. The left side of the reattached line was a separation zone. Both this separation zone and gap vortex of rotor formed a large flow loss region, in this flow condition, the flow losses of this three cascades had little difference.

Temperature distribution of HP blade tip at off-design condition: The static temperature nephogram of the three cascades at the up end wall was shown in Fig. 8. At the design flux condition, the inlet temperature of SWF stage cascades was high and SWB stage cascade had the lowest temperature. The

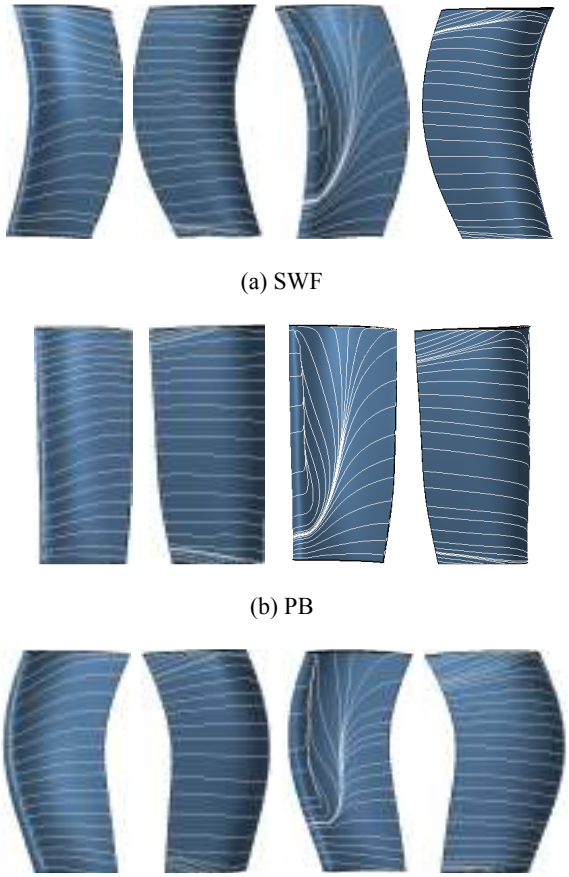

(a) SWF

(b) PB

(c) SWB

100% flow mass 50% flow mass

Fig. 7: HP stage rotor cascades surface streamline

temperature of SWF on the rotor pressure side increased more than that on SWB and PB, while the temperature of SWB decreased a little.

When the inlet flux of SWF cascade reached 50% design flux, compared to PB stage, the temperature on the rotor pressure side in the gap increased and the temperature increased zone on the suction side was decreased. For SWB stage, the temperature increased sharply at outlet of static blade cascade and the high temperature formed a big area even reached the rotor suction side. The temperature of SWB stage on rotor pressure side increased sharply too. When the inlet flux reached 120% design flux condition, compared to PB stage, the temperature of SWF tip changed a little, but the SWB's temperature decreased relatively.

Outlet flow angle variation of HP stage with mass flow at off-design condition: The three cascade pitch average flow angle distribution with the flow changes was shown in Fig. 9. The flow angle of SWB stage

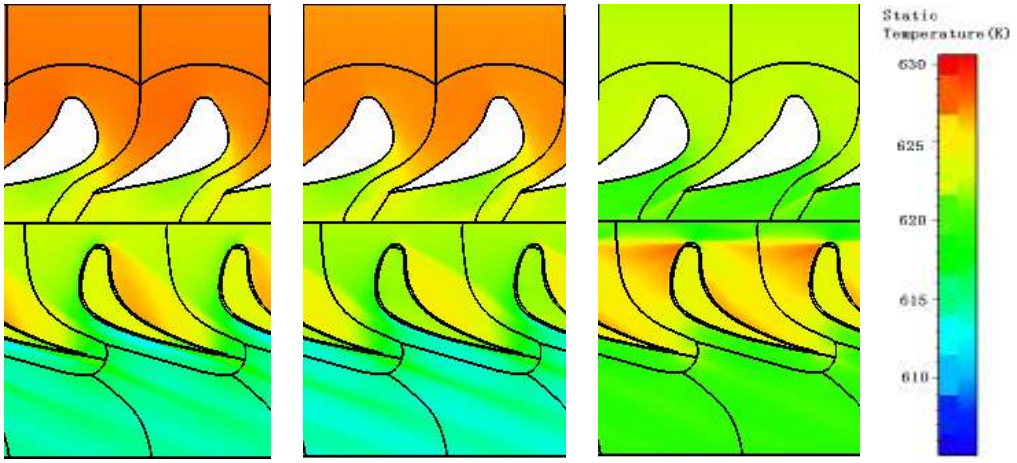

(a) SWF stage blade tip static temperature distribution

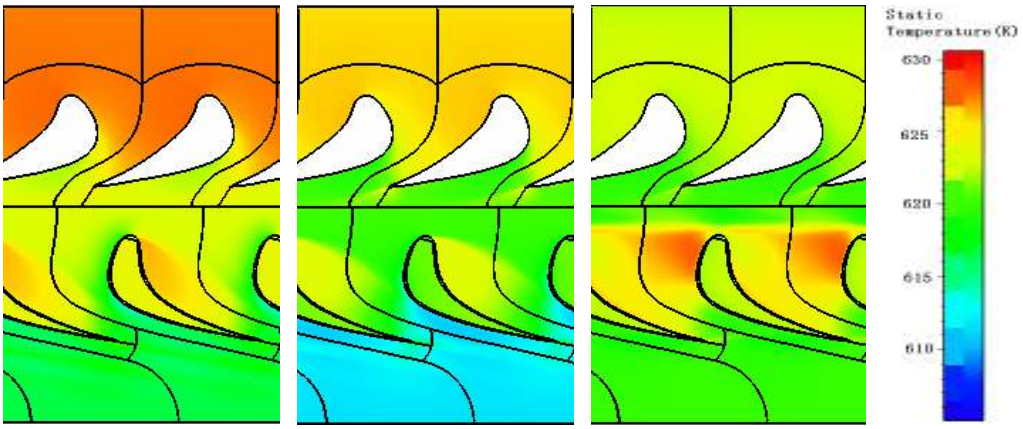

(b) PB stage blade tip static temperature distribution

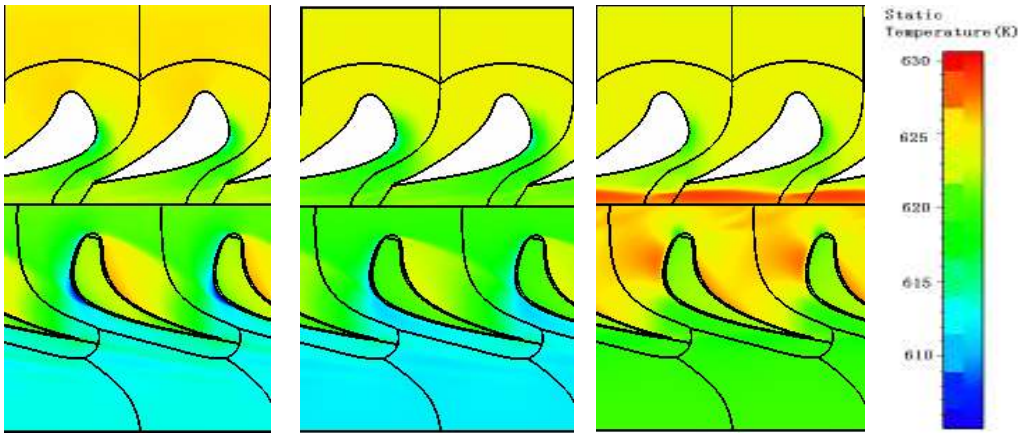

(c) SWB stage blade tip static temperature distribution

120% mass flow 100% mass flow 50% mass flow

Fig. 8: Static temperature contours of HP stage tip blade

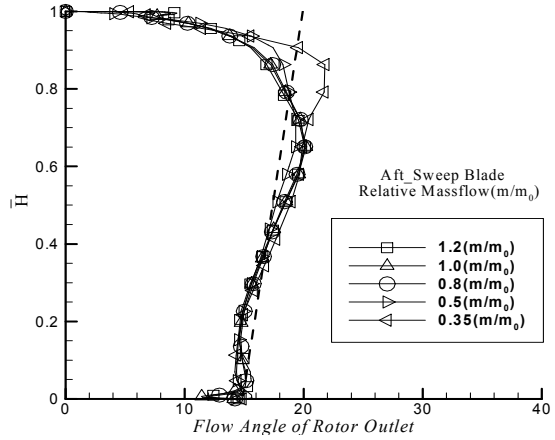

(a) SWB stage outlet flow angle

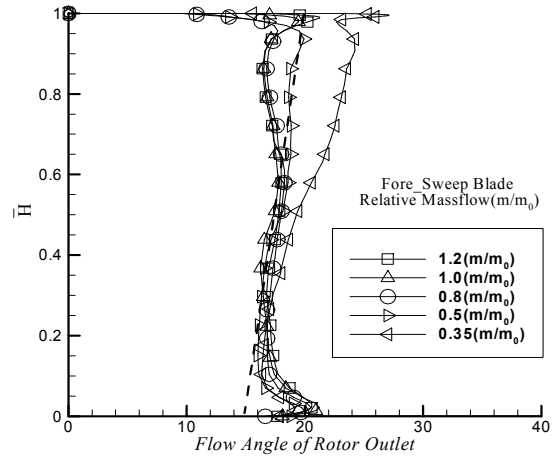

(b) SWF stage outlet flow angle

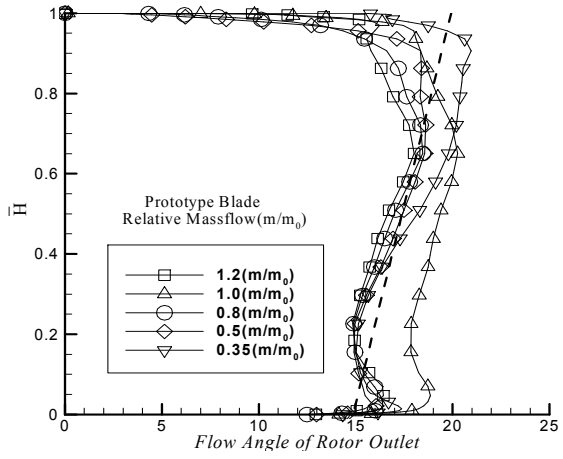

(c) PB stage outlet flow angle

Fig. 9: Pitchwise averaged outlet flow angle of HP stage rotor cascades

nearly didn't changed in the scope of 0~70% design flux but decreased obviously when the flux was increased to 70% design flux. The flow angle was decreased with flux decreasing. It was indicated that because the tip gap vortex was weaken, there was much fluid leakage. Flow angle of PB stage hardly changed in the scope of 0~40% blade height and decreased a little in the other blade height scope. The flow angle of SWF stage deviated from the design condition no matter how large or small flux and its less deflection was formed. The flow angle increased a little with inlet flux decreasing. The less deflection of flow angle was the most serious one at 120% design flux.

CONCLUSION

Based on the aerodynamic of turbo machinery, numerical simulation of the HP stages with different swept angles was conducted at off-design condition by MUNECA. The calculated results indicated:

The degree of reaction and isentropic efficiency of SWF, SWB and PB stages changed very little in the scope of 70~120% design flux. It indicated that the static cascades enthalpy drop was nearly equal to the rotor so that in steam turbine passage, the steam velocity changed gently and flow loss was very little, isentropic efficiency kept high value. When the flux was less than 50% design flux, the average degree of reaction and isentropic efficiency sharply decreased. With the inlet flux increasing, the stage's output power and axial thrust were also increased.

The streamline of three cascade stages were all nearly flow along the blade profile curve in the scope of 80~120% design flux. It was indicated that the flow in middle passage of any cascade stages were all laminar flow. When the inlet flux was less than 50% design flux, the streamline of rotor cascade was deflected to suction surface of rotor blade and formed negative incidence, at the same time, the secondary flow was formed in the pressure surface of rotor blade. The vortex of SWB was the largest, followed by PB, the SWF was the least. The vortex was enhanced with the flux decreasing.

NOMENCLATURE

A = Sweep Angle
H = Sweep Height
HP = High Pressure
Cps = Static Pressure coefficient = static pressure/ Incoming Total Pressure before cascade
PB = Prototype Blade
SWF = Chordwise fore-sweep blade
SWB = Chordwise aft-sweep blade

DR = Degree of reaction
X/B = Axial Relative Chord Length Coordinate
Cpt = Total Pressure Loss Coefficient
SS = Suction Surface
S = Pressure Surface
LE = Leading Edge
TE = Trailing Edge

REFERENCES

Ainley, D.G., 1948. The performance of axial flow turbines. Proc. Instn. Mechanical Engineers, 159(41): 230-237.

Corriveau, D. and S.A. Sjolander, 2005. Aerodynamic Performance of a Family of Three High Pressure Transonic Turbine Blades at Off-Design Incidence. ASME Paper GT-2005-68159, pp: 1-12.

Hournouziadis, B.F. and P. Bergmann, 1987. The development of the profile boundary layer in a turbine environment. J. Turbomach., 109(2): 286-295.

Jouini, D.B.M. and S.A. Ajolander, 2000. Aerodynamic Performance of a Transonic Turbine Cascade at Off-Design Conditions. ASME Paper 2000-GT-0482, pp: 1-14.

Mayle, R.E., 1991. The 1991 IGTI scholar lecture: The role of laminar-turbulent transition in gas turbine engines. ASME J. Turbomach., 113(4): 509-536.

Solomon, W.J., 2000. Effects of Turbulence and Solidity on the Boundary Layer Development in a Low Pressure Turbine. ASME Paper 2000-GT-0273, pp: 1-12.

Willinge, R.R. and H. Haselbacher, 2004. Axial Turbine Tip-Leakage Losses at Off-Design Incidences. ASME Paper GT-2004-53039, pp: 1-11.

Zoric, P. and S.A. Sjolander, 2007. Comparative Inve T. stigat I. ion of Three Highly Loaded Lp Turbine Airfoils: Part II-Measured Profile and Secondary Losses at Off-Design Incidence. ASME Paper GT-2007-27539.